

Electrochemical Characterization of Liquid Phase Exfoliated Two-Dimensional Layers of Molybdenum Disulfide

Andrew Winchester,[†] Sujoy Ghosh,[†] Simin Feng,[‡] Ana Laura Elias,[‡] Tom Mallouk,[§] Mauricio Terrones,^{‡,§,||} and Saikat Talapatra^{*,†}

[†]Department of Physics, Southern Illinois University, Carbondale, Illinois 62901, United States

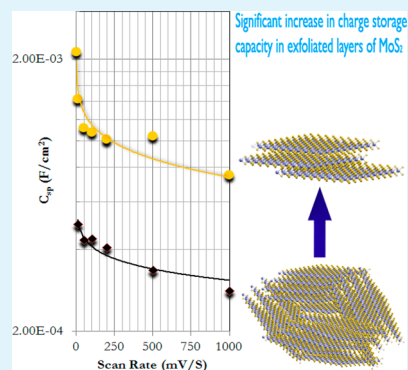
[‡]Department of Physics and Center for 2-Dimensional and Layered Materials, The Pennsylvania State University, University Park, Pennsylvania 16802, United States

[§]Department of Chemistry, The Pennsylvania State University, University Park, Pennsylvania 16802, United States

^{||}Department of Materials Science and Engineering, The Pennsylvania State University, University Park, Pennsylvania 16802, United States

ABSTRACT: We report on the electrochemical charge storage behavior of few-layered flakes of molybdenum disulfide (MoS₂) obtained by liquid phase exfoliation of bulk MoS₂ powder in 1-dodecyl-2-pyrrolidinone. The specific capacitances of the exfoliated flakes obtained using a 6 M KOH aqueous solution as an electrolyte were found to be an order of magnitude higher than those of bulk MoS₂ (~0.5 and ~2 mF cm⁻² for bulk and exfoliated MoS₂ electrodes, respectively). The exfoliated MoS₂ flakes also showed significant charge storage in different electrolytes, such as organic solvents [1 M tetraethylammonium tetrafluoroborate in propylene carbonate (Et₄NBF₄ in PC)] and ionic liquids [1-butyl-3-methylimidazolium hexafluorophosphate (BMIM-PF₆)]. The values of specific capacitances obtained using Et₄NBF₄ in PC and BMIM-PF₆ were ~2.25 and ~2.4 mF cm⁻², respectively. An analysis of electrochemical impedance spectroscopy using an equivalent circuit modeling was performed to understand the charge storage mechanism of these exfoliated MoS₂ flakes using different electrolytes. Our findings indicate that liquid phase exfoliation methods can be used to produce large quantities of electrochemically active, two-dimensional layers of MoS₂ and can act as an ideal material in several applications related to electrochemistry.

KEYWORDS: 2D layered materials, molybdenum disulfide, liquid phase exfoliation, electrochemical, charge storage



INTRODUCTION

Molybdenum disulfide (MoS₂) is an indirect band gap semiconductor that belongs to the group VI family of transition metal dichalcogenides (TMDs). The crystalline structure of this material, consisting of stacked S–Mo–S sheets, gives rise to various physicochemical properties ranging from solid lubricants to catalysts. For example, crystals of MoS₂ have been known to be a photoactive material; early work by H. Tributsch established that MoS₂ crystals, along with other semiconducting TMDs such as MoSe₂ and WSe₂, could be used as stable photoelectrochemical electrodes.^{1,2} Subsequent work on polycrystalline thin films of MoS₂ showed a comparable photoelectric response similar to that of single crystals.^{3,4} More recently, methods for producing thinner films with larger yields via intercalation, exfoliation, and chemical means have been explored.^{5–10} MoS₂ has also been evaluated as a photocatalyst for the production of H₂ gas, with potential for becoming a lower-cost replacement for platinum.^{6,11–13}

As described above, bulk crystals of MoS₂ are known to have an indirect band gap of ~1.2–1.3 eV,^{14,15} which has led to much of the initial photoelectrical research on this material. However, because of its layered structure, it is possible to

exfoliate this system into fewer layers and observe significant changes in its physical and chemical properties. For example, it has been shown both theoretically and experimentally that via isolation of individual layers of the crystal, significant changes in the band structure of MoS₂ are observed. In particular, a direct band gap of ~1.7–1.9 eV is opened in monolayer MoS₂.^{16–18} Therefore, it is important to study the influence of the number of layers and the addition of edges in MoS₂ on the photocatalytic efficiency of evolving hydrogen gas.^{11,13} Recently, it has been demonstrated that with an increase in the available surface area from the bulk crystal to few or single layers of MoS₂, it is possible to observe enhanced charged storage in lithium ion battery systems^{19,20} and supercapacitors.^{21–23} Therefore, it is very important to control the number of layers, the amount of reactive edges, and defects within these semiconducting TMDs to fabricate the next generation of energy-storage and -harvesting systems.

Received: November 20, 2013

Accepted: January 20, 2014

Published: January 20, 2014

In this work, we study fundamental electrochemical properties of MoS₂ exfoliated into few-layer stacks by examining the behavior of the resulting material in different electrolytes. Our findings indicate that upon exfoliation, the electrochemical charge storage capacity of these layered systems increases by an order of magnitude compared to that of their bulk counterpart when measured in different electrolytes (KOH, Et₄NBF₄ in PC, and BMIM-PF₆). We obtained a maximal specific capacitance of ~2.4 mF cm⁻² with BMIM-PF₆ as the electrolyte (applied voltage window of 3.5 V). Electrochemical impedance spectroscopy (EIS) in conjunction with circuit analysis indicates that in an aqueous electrolyte (e.g., KOH), nearly pure capacitive behavior is observed in the charge storage mechanism, whereas for polymers and other ionic electrolytes, diffusive behavior is more prevalent.

EXPERIMENTAL SECTION

The few-layer MoS₂ dispersions were obtained via a liquid phase exfoliation technique, as reported by Coleman et al.^{24,25} Commercial MoS₂ powder (Sigma Aldrich, <2 μm) was added to 1-dodecyl-2-pyrrolidinone (N12P) at a concentration ratio of approximately 10 mg/mL. The mixture was then treated ultrasonically using a Fisher Scientific Sonic Dismembrator 500 horn tip sonicator operating between 20 and 40% amplitude. The dispersions were treated for 1 h continuously using an ice/water bath to maintain a stable temperature for the solution. After this ultrasonic treatment, the dispersions were centrifuged at 1500 rpm for 45 min and then decanted, thus forming a uniform suspension (Figure 1a). UV-vis spectra were recorded using a Perkin Elmer Lambda 25 spectrophotometer (Figure 1b). The wavelength was scanned from 800 to 300 nm in 1 nm steps. Transmission electron microscopy (TEM) imaging was conducted using a Hitachi 7650 transmission electron microscope operating at 60 kV. Electrochemical characterization measurements were conducted

with a Princeton 2263 model potentiostat using a two-electrode parallel-plate-type arrangement. Cyclic voltammetry (CV) measurements were performed at scan rates between 10 and 500 mV s⁻¹ with vertex potentials of -0.8 to 0.2 V (KOH), -1.0 to 1.7 V (Et₄NBF₄), and -2.0 to 1.5 V (BMIM-PF₆). Galvanostatic charge-discharge was performed with charging and discharging intervals of 1.0 s at constant currents of 0.1 mA (aqueous and organic) and 1.0 mA (ionic liquid). Electrochemical impedance spectroscopy (EIS) measurements were performed using a 10 mV RMS ac signal and no dc bias over frequency ranges of 100 kHz to 100 mHz (KOH), 1 MHz to 10 mHz (Et₄NBF₄), and 1 MHz to 100 mHz (BMIM-PF₆).

RESULTS AND DISCUSSION

In Figure 1, the structural characterization and optical characterization of the exfoliated MoS₂ flakes are shown. Figure 1a shows a typical dispersion of MoS₂ flakes in N12P. A representative UV-vis spectrum of such a dispersion displaying the region from 400 to 800 nm is shown in Figure 1b. This region clearly displays the A and B peaks centered at ~680 nm (1.83 eV) and ~620 nm (1.99 eV), respectively. The peaks are due to exciton splitting and show a separation of ~60 nm (~0.16 eV), which is characteristic of the 2H-MoS₂ phase.^{7,15,26} The spectrum also displays the broader C absorption peak located at ~455 nm (2.73 eV) and possibly also the D absorption peak (typically between ~400 and ~450 nm), although these peaks are largely masked by the significant scattering background at higher frequencies in this sample. These indicate that the structure of the MoS₂ sheets is left largely intact during the exfoliation process. Via further examination of the absorbance data via means of a Tauc plot,²⁷ the band gap of the material can be estimated. Analysis of the Tauc plot in the linear absorbing region (Figure 1b, inset) gives a value of ~1.75 eV for the direct band gap, which agrees with theoretical and experimental values reported in the literature for few-layer MoS₂.^{16-18,26} Therefore, from the optical band gap value obtained from the UV-vis analysis, we can perhaps assume that the exfoliation results in MoS₂ flakes containing three or four layers.

Panels c and d of Figure 1 illustrate TEM micrographs of the exfoliated MoS₂ flakes. TEM samples were prepared by directly dropping small amounts of the dispersions onto holey-carbon-coated grids. The grids were allowed to completely dry in an oven at 60 °C before being imaged. An electron diffraction pattern from one of the MoS₂ flakes, shown in Figure 1d, is also presented in the inset. From the ED data, it is extremely difficult to say if the samples obtained using this process have stacked multilayers with rotated stacking or are stacked in-layer multidomain materials, but in general, it can be assumed that because the samples are exfoliated from bulk MoS₂ powder, which are typically in-layer multidomain material, we believe that the exfoliated samples are perhaps in-layer multidomain material. In any event, the crystalline nature of the flakes is evident from this diffraction pattern.

In Figure 2, we show data obtained from our electrochemical measurements. The electrochemical behavior of exfoliated MoS₂ was studied by constructing two electrodes in a parallel-plate geometry, as is typically used in electrochemical double-layer capacitor (EDLC) measurements. Electrodes for these EDLCs were fabricated by vacuum filtering small portions of the dispersions, approximately 1–10 mL, through thin Teflon filters (Millipore) to create thin, flexible films of MoS₂. The filters were then cut into small pieces, of areas ranging between ~0.25 and ~0.5 cm², and were then pressed together with a porous separator (Ahlstrom Qualitative Filter Paper)

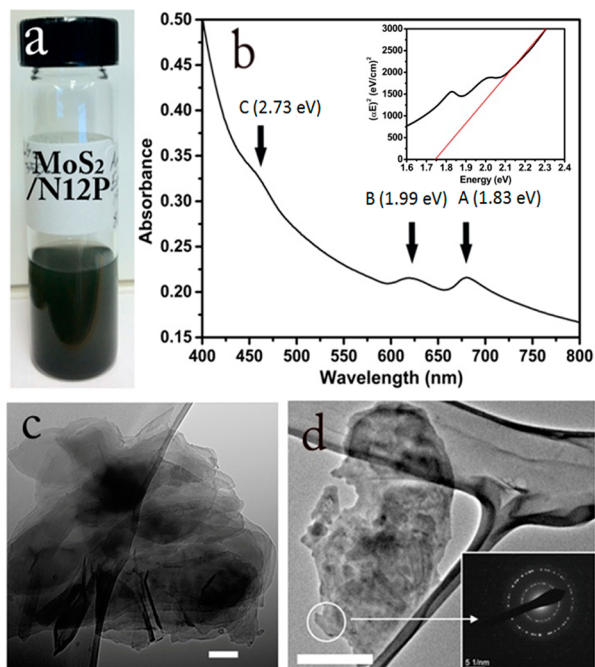


Figure 1. (a) Optical image of a dispersion of exfoliated MoS₂. (b) UV-vis spectrum of exfoliated MoS₂ showing characteristic peaks with the corresponding values in electronvolts. The inset displays a Tauc plot with linear extrapolation, giving a direct band gap of ~1.75 eV. (c) TEM image of a stack of thin flakes of exfoliated MoS₂. (d) TEM image of a small, few-layer flake of MoS₂, with the inset showing the electron diffraction pattern showing the crystalline structure.

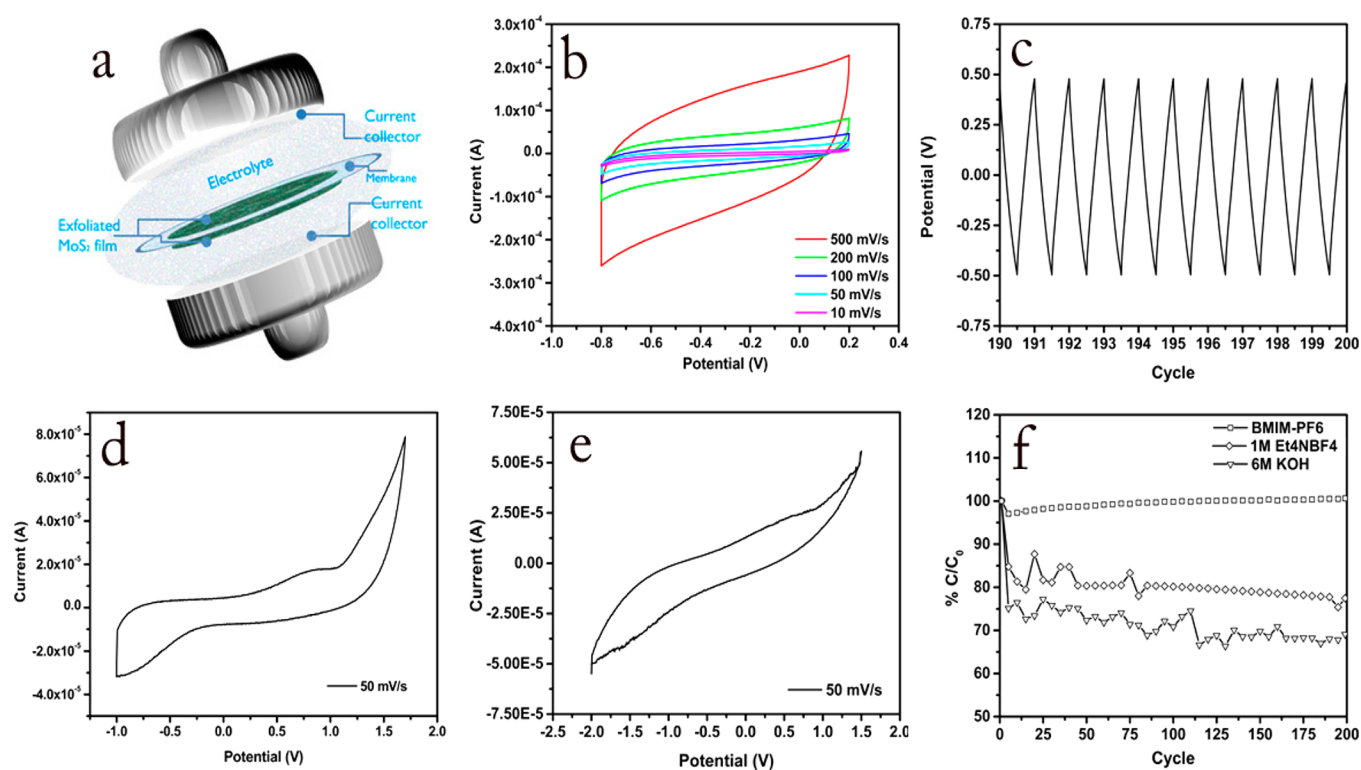


Figure 2. (a) Exploded view of the geometry used to prepare EDLC devices. (b) Cyclic voltammetry at various scan rates of a MoS₂ EDLC using KOH as the electrolyte. (c) Charge–discharge cycles for the MoS₂ EDLC using KOH as the electrolyte. (d) Cyclic voltammetry at a scan rate of 50 mV s⁻¹ for a system using Et₄NBF₄ as the electrolyte. (e) Cyclic voltammetry at a scan rate of 50 mV s⁻¹ for a system using BMIM-PF₆ as the electrolyte. (f) Plot of the percent capacitance retained as a function of the number of cycles for each of the electrolytes.

into a thin sandwich, an “exploded” view of which is shown in Figure 2a. Measurements were then performed inside a sealed electrochemical stainless steel cell with the polished stainless steel current collectors of the cell making direct electrical contact with the sample material to create a parallel-plate geometry. Electrochemical measurements using 6 M potassium hydroxide (KOH) as the electrolyte indicated excellent cyclic voltammetry (CV) responses (Figure 2b) with nearly rectangular curves, even at higher scan rates. The CV responses of the system lack any noticeable peaks that would indicate oxidation or reduction processes.²⁸ Galvanostatic charge–discharge was also performed, showing good long-term device stability, nearly linear charging and discharging, and very little IR drop during discharge (Figure 2c).

Values for the capacitance were calculated from the CV curves using the relation $C_{sp} = \int idV / (sA\Delta V)$, where the integral provides the area of the CV curve, s is the scan rate for the particular curve, A is the area of a single electrode exposed to the electrolyte, and ΔV is the applied potential window through which the device is scanned. The highest value calculated for KOH at a scan rate of 10 mV s⁻¹ was ~ 2 mF cm⁻². This value is at least 1 order of magnitude higher than the values obtained using bulk MoS₂ as EDLC electrodes (~ 0.5 mF cm⁻²). This also indicates that exfoliation results in an increase in the specific surface area of the MoS₂ (by at least 1 order of magnitude) because double-layer capacitance is proportional to specific surface area. The typical surface area of bulk MoS₂ is ~ 30 m² g⁻¹; therefore, we can estimate the specific surface areas of the exfoliated samples to be on the order of a few hundreds of square meters per gram. The capacitance was also calculated from the charge–discharge curves using the relation $C_{sp} = I / (A \times dV/dt)$, where I is the constant discharge current,

A is the area of a single electrode exposed to the electrolyte, and dV/dt is the slope of the discharge curve, giving values that typically agreed with that from CV measurements.

Electrochemical characterization of MoS₂ electrodes was further investigated using two additional electrolytes: 1 M tetraethylammonium tetrafluoroborate in propylene carbonate (Et₄NBF₄ in PC) and 1-butyl-3-methylimidazolium hexafluorophosphate (BMIM-PF₆). EDLC electrodes were prepared in the same manner as indicated above. Cyclic voltammetry, galvanostatic charge–discharge, and electrochemical impedance spectroscopy characterization were conducted for each electrolyte, again showing capacitive behavior. The CV curves (Figure 2d,e) are much less rectangular and symmetric than those of the KOH-based EDLCs. This is likely due to effects from resistive leaking, often seen in EDLC devices. In particular, the CV curves for the Et₄NBF₄ display a rather sharp, asymmetric peak starting at approximately 1 V. This rapid increase in current occurs for several reasons; for example, the surface roughness of the electrodes can lead to charge puddles that might show jumps in the current during CV measurements. Further, the humidity level can also slightly influence the CV measurements because Et₄NBF₄ is known to readily absorb water from its surroundings. The charge–discharge curves for all three electrolytes display only small losses of retained capacitance over numerous cycles (Figure 2f), leading to these systems showing good device stability. Here we note that the data presented in Figure 2f are from the first set of measurements of the EDLC devices. The electrodes were not conditioned before the cycling. The initial loss of capacitance during the first few cycles is perhaps due to the time required for the system to attain electrochemical stability. Calculations of the capacitance for a scan rate of 10 mV s⁻¹ give values of

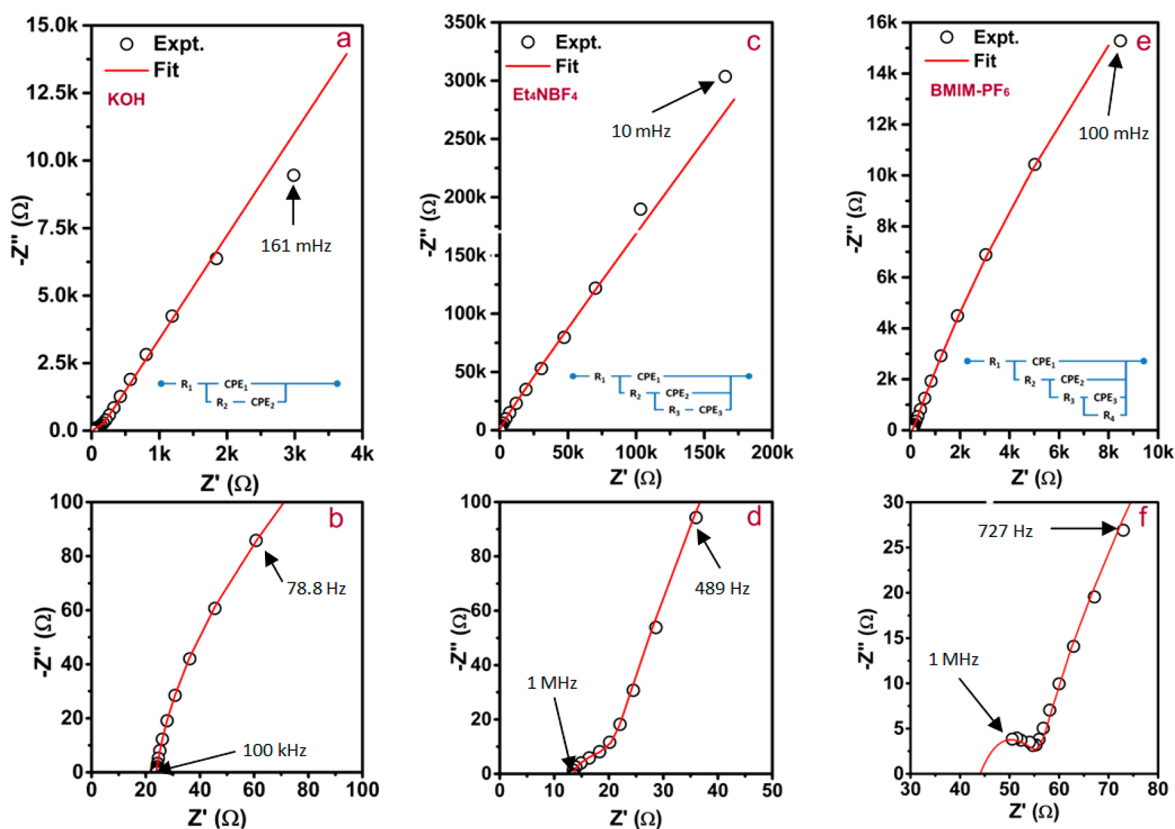


Figure 3. Experimental and fitted EIS spectra with equivalent circuit inset for KOH (a), Et_4NBF_4 (c), and BMIM- PF_6 (e). High-frequency intercepts are shown in panels b, d, and f for KOH, Et_4NBF_4 , and BMIM- PF_6 , respectively.

~ 2.25 and ~ 2.4 mF cm^{-2} for Et_4NBF_4 and BMIM- PF_6 , respectively.

The values of specific capacitances obtained for our samples are comparable to the values of specific capacitances obtained in a very recent study by Cao et al.,²² for hydrothermally prepared as well as exfoliated MoS_2 materials. They have shown that MoS_2 prepared by hydrothermal methods can be used for preparing EDLC electrodes by utilizing laser patterning to create small electrode feature sizes with areal capacitances of 8 mF cm^{-2} at a scan rate of 10 mV s^{-1} in aqueous electrolytes. In this work, MoS_2 prepared via a liquid phase exfoliation method was also studied, showing a capacitance of ~ 3.1 mF cm^{-2} . Previous work on MoS_2 by Soon et al.²¹ showed that edge-oriented nanowall films of MoS_2 can show extraordinary pseudocapacitance in a number of active redox systems at very low scan rates. As in this work, however, we do not see characteristics of Faradic charge transfer with aqueous electrolytes at higher scan rates between 10 and 500 mV s^{-1} . Other recent work, performed by Huang et al.,²³ showed that hydrothermally prepared composites of MoS_2 and polyaniline work together in a synergistic way to achieve very high capacitances (~ 575 F g^{-1}) with very stable devices (loss of $\sim 2\%$ capacitance over 500 cycles) in an aqueous environment (1 $\text{M H}_2\text{SO}_4$). This work gives a perspective on how these materials can be utilized in different ways to make optimal use of their properties.

To further characterize these samples, electrochemical impedance spectroscopy (EIS) was utilized. The impedance spectrum of the KOH device was acquired within the frequency (f) range of 100 kHz to 100 mHz with a 10 mV RMS voltage and no dc bias. The resulting Nyquist plot of the real and

imaginary parts of the impedance, shown in Figure 3a, could be used to directly estimate the equivalent series resistance (ESR) of the device.^{28,29} Looking at the high-frequency intercept of the real axis for the KOH-based system (Figure 3b), for example, gives a value of approximately 23.9 Ω for the ESR. To gain deeper insight, the impedance spectrum can be fit to an equivalent circuit; a suitable circuit can give some general idea about what physical processes may be occurring in the system.^{28,30} A simple circuit (inset of Figure 3a), similar to a Randles circuit,²⁸ was found to represent the KOH-based system for a wide range of frequencies. The presence of a constant phase element (CPE) corresponds to nonideal capacitor behavior; CPEs are frequently used to represent system behavior due to effects such as surface disorder, electrode porosity, and adsorption processes.³¹ This is likely caused by the electrode being comprised of random stacks of MoS_2 sheets, creating a very disordered surface geometry with a large distribution of pore sizes. The R_1 resistor element is the device ESR corresponding to the series resistance of the electrolyte, filter papers, and charge barriers between the stainless steel current collectors and the MoS_2 electrode material. The R_2 resistor element is most likely due to a charge transfer barrier in the system.^{28,31} The presence of a second constant phase element could be attributed to a very small contribution to the total capacitance from a pseudocapacitance process, such as the adsorption of ions onto the electrode.^{28,31} When the impedance spectra for the Et_4NBF_4 (Figure 3c,d) and BMIM- PF_6 (Figure 3e,f) electrolytes were fit, it was found that simple modifications to the circuit for the KOH-based system allow the more complicated behavior of the organic and ionic electrolytes to be modeled. The presence of

an additional constant phase element and resistors leads to a model very similar to that of the ideal transmission line model of a porous electrode containing a series of RC elements in parallel,²⁸ with the BMIM-PF₆-based electrolyte displaying a leakage pathway through a R₄ resistor element. This additional “RCPE” element perhaps corresponds to a part of the system with a different relaxation time, caused by mobility differences of anions and cations or to processes such as adsorption of ions onto the electrodes.^{28,31}

To further compare the models to experimental data, the capacitance from the constant phase elements was calculated. Using the relation $C = P/[f^{1-n} \times \sin(n\pi/2)]$, where P and n are fitting parameters and f is taken to be the lowest frequency measured in the impedance spectrum, allows for the individual contributions to the total capacitance to be calculated. The total calculated values matched the values found experimentally (see Table 1). The fitting parameter values could also be used to

Table 1. Impedance Spectra Fitting Parameters with Calculated Capacitances

	KOH	Et ₄ NBF ₄	BMIM-PF ₆
R ₁ (ESR) (Ω)	23.908	13.669	43.832
R ₂ (Ω)	279.85	15.152	12.619
R ₃ (Ω)	not applicable	38.324	121.23
R ₄ (Ω)	not applicable	not applicable	125480
P ₁	3.1198 × 10 ⁻⁵	9.0641 × 10 ⁻⁷	2.4362 × 10 ⁻⁶
n ₁	0.91348	1	0.6779
P ₂	7.1717 × 10 ⁻⁵	1.8373 × 10 ⁻⁶	3.5472 × 10 ⁻⁵
n ₂	0.80817	1	0.77989
P ₃	not applicable	1.650 × 10 ⁻⁵	4.1587 × 10 ⁻⁵
n ₃	not applicable	0.63268	0.77438
CPE ₁ capacitance (F)	3.843 × 10 ⁻⁵	9.0641 × 10 ⁻⁷	5.847 × 10 ⁻⁶
CPE ₂ capacitance (F)	1.168 × 10 ⁻⁴	1.8373 × 10 ⁻⁶	6.259 × 10 ⁻⁵
CPE ₃ capacitance (F)	not applicable	1.069 × 10 ⁻⁴	7.455 × 10 ⁻⁵
total capacitance (F)	1.552 × 10 ⁻⁴	1.096 × 10 ⁻⁴	1.430 × 10 ⁻⁴
experimental capacitance (F)	2.78 × 10 ⁻⁴ @ 1000 mV s ⁻¹	1.93 × 10 ⁻⁴ @ 1000 mV s ⁻¹	1.90 × 10 ⁻⁴ @ 200 mV s ⁻¹

glean some further insight into the systems. Notably, the values for n provide some information about the capacitive behavior occurring at the electrodes. The value of n indicates how “pure” the capacitive behavior is; a value of n equal to 1 gives ideal capacitor behavior.³¹ The relatively higher values of n for the KOH-based device when compared to those of the other two electrolytes could be related to ion size and surface accessibility: KOH ions are smaller than the bulky organic ions of the other two electrolytes and can therefore access the MoS₂ surface area more readily. The lower value for n in the BMIM-PF₆ and Et₄NBF₄ electrolyte systems indicates that a diffusive behavior is more prevalent.³¹ A comparison of several values related to the modeled circuit for each electrolyte and values of capacitances obtained from our experimental measurements are listed in Table 1.

CONCLUSION

We have demonstrated the effect of exfoliation on the electrochemical charge storage behavior as well as electrochemical interaction of MoS₂ with different electrolytes. A systematic investigation of electrochemical properties in

aqueous, organic, and ionic electrolytes has shown a significant increase in the charge storage capacities of two-dimensional (2D) layers obtained via exfoliation compared to those of bulk powders. The mechanism of the charge storage process for each electrolyte was examined through electrochemical impedance spectroscopy, revealing that these systems show a predominantly physical charge storage process. The random nature of the restacked MoS₂ electrodes also leads to diffusive behavior in these systems. While exfoliated MoS₂ flakes by themselves as an electrode material have shown only modest results thus far, their ability to act in redox systems boosts their potential applications. We believe that exfoliated materials obtained and studied in this work can further be utilized in creating functional composites, similar to work done on hydrothermally prepared MoS₂. These findings indicate that an exfoliation process could lead to large scale synthesis of electrochemically active 2D layer materials, which could have a significant impact in several applications related to electrochemical processes such as electrochemical catalysis as well as photocatalytic applications.

AUTHOR INFORMATION

Corresponding Author

*E-mail: stalapatra@physics.siu.edu. Phone: (618) 453-2270. Fax: (618) 453-1056.

Notes

The authors declare no competing financial interest.

ACKNOWLEDGMENTS

This work was supported by U.S. Army Research Office MURI Grant W911NF-11-1-0362.

ABBREVIATIONS

MoS₂, molybdenum disulfide
 N12P, 1-dodecyl-2-pyrrolidinone
 Et₄NBF₄, tetraethylammonium tetrafluoroborate
 BMIM-PF₆, 1-butyl-3-methylimidazolium hexafluorophosphate
 EIS, electrochemical impedance spectroscopy
 KOH, potassium hydroxide
 UV-vis, ultraviolet-visible
 EDLC, electrochemical double-layer capacitor
 CV, cyclic voltammetry
 CPE, constant phase element

REFERENCES

- (1) Tributsch, H. *Faraday Discuss.* **1980**, *70*, 189–205.
- (2) Kautek, W.; Gerischer, H.; Tributsch, H. *J. Electrochem. Sci. Technol.* **1980**, *127*, 11.
- (3) Schneemeyer, L. F.; Cohen, U. *J. Electrochem. Sci. Technol.* **1983**, *130*, 7.
- (4) Cabrera, C. R.; Abruña, H. D. *J. Electrochem. Sci. Technol.* **1988**, *135*, 6.
- (5) Santiago, Y.; Cabrera, C. R. *J. Electrochem. Soc.* **1994**, *141*, 3.
- (6) Ho, W.; Yu, J. C.; Lin, J.; Yu, J.; Li, P. *Langmuir* **2004**, *20*, 5865–5869.
- (7) Eda, G.; Yamaguchi, H.; Vohry, D.; Fujita, T.; Chen, M.; Chhowalla, M. *Nano Lett.* **2011**, *11*, 5111–5116.
- (8) Wu, S.; Zeng, Z.; He, Q.; Wang, Z.; Wang, S. J.; Du, Y.; Yin, Z.; Sun, X.; Chen, W.; Zhang, H. *Small* **2012**, *8* (14), 2264–2270.
- (9) Liu, Y. D.; Ren, L.; Qi, X.; Yang, L. W.; Hao, G. L.; Li, J.; Wei, X. L.; Zhong, J. X. *J. Alloys Compd.* **2013**, *571*, 37–42.
- (10) King, L. A.; Zhao, W.; Chhowalla, M.; Riley, D. J.; Eda, G. *J. Mater. Chem. A* **2013**, *1*, 8935.

- (11) Jaramillo, T. F.; et al. *Science* **2007**, *317*, 100.
- (12) Xiang, Q.; Yu, J.; Jaroniec, M. *J. Am. Chem. Soc.* **2012**, *134*, 6575–6578.
- (13) Chen, Z.; Forman, A. J.; Jaramillo, T. F. *J. Phys. Chem. C* **2013**, *117*, 9713–9722.
- (14) Kam, K. K.; Parkinson, B. *J. Phys. Chem.* **1982**, *86*, 463.
- (15) Böker, Th.; Severin, R.; Müller, A.; Janowitz, C.; Manzke, R. *Phys. Rev. B* **2001**, *64*, 235305.
- (16) Mak, K.; Lee, C.; Hone, J.; Shan, J.; Heinz, T. *Phys. Rev. Lett.* **2010**, *105*, 136805.
- (17) Kadantsev, E. S.; Hawrylak, P. *Solid State Commun.* **2012**, *152*, 909–913.
- (18) Garadkara, K. M.; Patil, A. A.; Hankarea, P. P.; Chateb, P. A.; Sathe, D. J.; Delekar, S. D. *J. Alloys Compd.* **2009**, *487*, 786–789.
- (19) Chang, K.; Chen, W. *J. Mater. Chem.* **2011**, *21*, 17175.
- (20) Chang, K.; Chen, W. *ACS Nano* **2011**, *5* (6), 4720–4728.
- (21) Soon, J. M.; Loh, K. P. *Electrochem. Solid-State Lett.* **2007**, *10* (11), A250–A254.
- (22) Cao, L.; Yang, S.; Gao, W.; Liu, Z.; Gong, Y.; Ma, L.; Shi, G.; Lei, S.; Zhang, Y.; Zhang, S.; Vajtai, R.; Ajayan, P. M. *Small* **2013**, *9*, 2905–2910.
- (23) Huang, K. J.; Wang, L.; Liu, Y. J.; Wang, H. B.; Liu, Y. M.; Wang, L. L. *Electrochim. Acta* **2013**, *109*, 587–594.
- (24) Coleman, J. N.; et al. *Science* **2011**, *331*, 568.
- (25) O'Neill, A.; Khan, U.; Coleman, J. N. *Chem. Mater.* **2012**, *24*, 2414–2421.
- (26) Coehoorn, R.; Haas, C.; de Groot, R. A. *Phys. Rev. B: Condens. Matter Mater. Phys.* **1987**, *35*, 12.
- (27) Dholakia, D. A.; Solanki, G. K.; Patel, S. G.; Agarwal, M. K. *Bull. Mater. Sci.* **2001**, *24* (3), 291–296.
- (28) Conway, B. E. *Electrochemical Supercapacitors: Scientific Fundamentals and Technological Applications*; Kluwer Academic/Plenum: Dordrecht, The Netherlands, 1999.
- (29) Kötz, R.; Hahn, M.; Gally, R. *J. Power Sources* **2006**, *154* (2), 550–555.
- (30) Macdonald, J. R. *Ann. Biomed. Eng.* **1992**, *20*, 289–305.
- (31) Jorcin, J.; Orazemb, M. E.; Pébère, N.; Tribollet, B. *Electrochim. Acta* **2006**, *51*, 1473–1479.